Journal of Hydrology: Regional Studies 38 (2021) 100939

Contents lists available at ScienceDirect

Journal of Hydrology: Regional Studies

journal homepage: www.elsevier.com/locate/ejrh

Real-time optimization of a large-scale reservoir operation in Thailand using adaptive inflow prediction with medium-range ensemble precipitation forecasts

Thatkiat Meema *, Yasuto Tachikawa, Yutaka Ichikawa, Kazuaki Yorozu

Department of Civil and Earth Resources Engineering, Kyoto University, Kyoto, Japan

ARTICLE INFO

Keywords:
Ensemble inflow forecasting
Data assimilation
Distributed hydrologic model
Reservoir optimization
Dynamic programing
Thailand

ABSTRACT

Study region: The Sirikit Dam in the Nan River Basin is located on a main tributary of the Chao Phraya River in Thailand.
Study focus: This study investigates forecasting river flows and real-time optimization of dam release using a distributed hydrological model with ensemble weather forecasting for reservoir operations which provide hydropower and irrigation facilities in Thailand during a case study of the 2019 drought event. Medium-range ensemble precipitation forecasts were employed using a hydrological model to predict the real-time reservoir inflow. Real-time optimization of the water release strategy determined a week in advance with an effective initial condition for hydropower generation and irrigation was conducted with different scenarios using dynamic programming considering inflow predictions.
New hydrological insights for the region: The medium-range ensemble precipitation forecast conducted by the European Centre for Medium Range Weather Forecasts was used to quantify precipitation for the study basin. The ensemble precipitation forecast with the hydrological model was employed for inflow prediction of the study basin which was located in a tropical climate with a distinct wet and dry season. The initial conditions of the hydrological model largely influenced the real-time inflow forecast. To determine the initial conditions of the model, the empirical data assimilation considering a drainage area factor was utilized and observed precipitation data were used for model input forcing data during the initial analysis period. This method improved the reservoir inflow prediction and real-time reservoir optimization using dynamic programming with considering ensemble forecasts provided more efficient operating decisions than employing historical data. The resulting information will be useful for water resource management, which may be adapted to other basins in the study region.

1. Introduction

The Sirikit Dam is one of the two large reservoirs in the Chao Phraya River Basin (CPRB) that is the largest (158,000 km^2) and most important in Thailand. The Sirikit reservoir, containing 9510 million m^3 of the total storage volume, has a significant role in effectively managing the water resources of the basin. However, the dam is located in a tropical climate with significant seasonal differences and uncertainty regarding the basin's hydrological condition influenced by both the Indian and Pacific Oceans (Nguyen et al., 2020). In

* Correspondence to: Department of Civil and Earth Resources Engineering, Kyoto University, C1, Nishikyo-ku, Kyoto 615-8540, Japan.
E-mail address: meema.thatkiat.42r@st.kyoto-u.ac.jp (T. Meema).

https://doi.org/10.1016/j.ejrh.2021.100939
Received 18 August 2021; Received in revised form 29 September 2021; Accepted 4 October 2021
Available online 7 October 2021

turn, these conditions cause both floods and droughts (Sayama et al., 2015), like the 2011 flood event, and the 2015 and 2019 drought events, which proved to be very challenging for reservoir operators. These uncertainties regarding the basin's hydrological condition have a primary effect on reservoir operation, increasing the risk of water disaster (Tingsanchali and Boonyasirikul, 2006). In addition, climate change complicates future water resource management in CPRB because of increasing extreme weather fluctuations (Kotsuki et al., 2014; Wichakul et al., 2015).

Incorporating weather forecast may improve the efficiency of decision making (Hamlet et al., 2002; Lettenmaier and Wood, 1993; Zhu et al., 2002). However, the forecast has limitations in accuracy (forecast uncertainty) with increasing forecast lead time. The optimum solution to capture and reduce this forecast error (uncertainty) is to use an ensemble forecast rather than a single (deterministic) forecast, because the ensemble forecast produces a set of randomly-equally-likely (independent) solutions for the future (Zhu, 2005).

In recent decades, ensemble forecast techniques have been rapidly developed. Ensemble forecast techniques are now generally accepted as a reliable approach for estimating forecast confidence, especially for high-impact weather (Bougeault et al., 2010). Based on these advantages, several studies have been conducted using ensemble forecast data, such as storm track prediction (Lin et al., 2020; Nishimura and Yamaguchi, 2015; Weber, 2003), reservoir inflow prediction (Fan et al., 2015), river flow prediction, and flood forecasting (Alfieri et al., 2012; Bao et al., 2011; He et al., 2010; Sayama et al., 2020).

Combining with using ensemble forecast information in a reservoir operation study, the dynamic programming (DP) is a well-known method to construct a mathematical model for decision support (Alemu et al., 2011). A number of studies have been conducted regarding ensemble streamflow predictions (ESP) with DP to improve reservoir operation efficiency. Faber and Stedinger

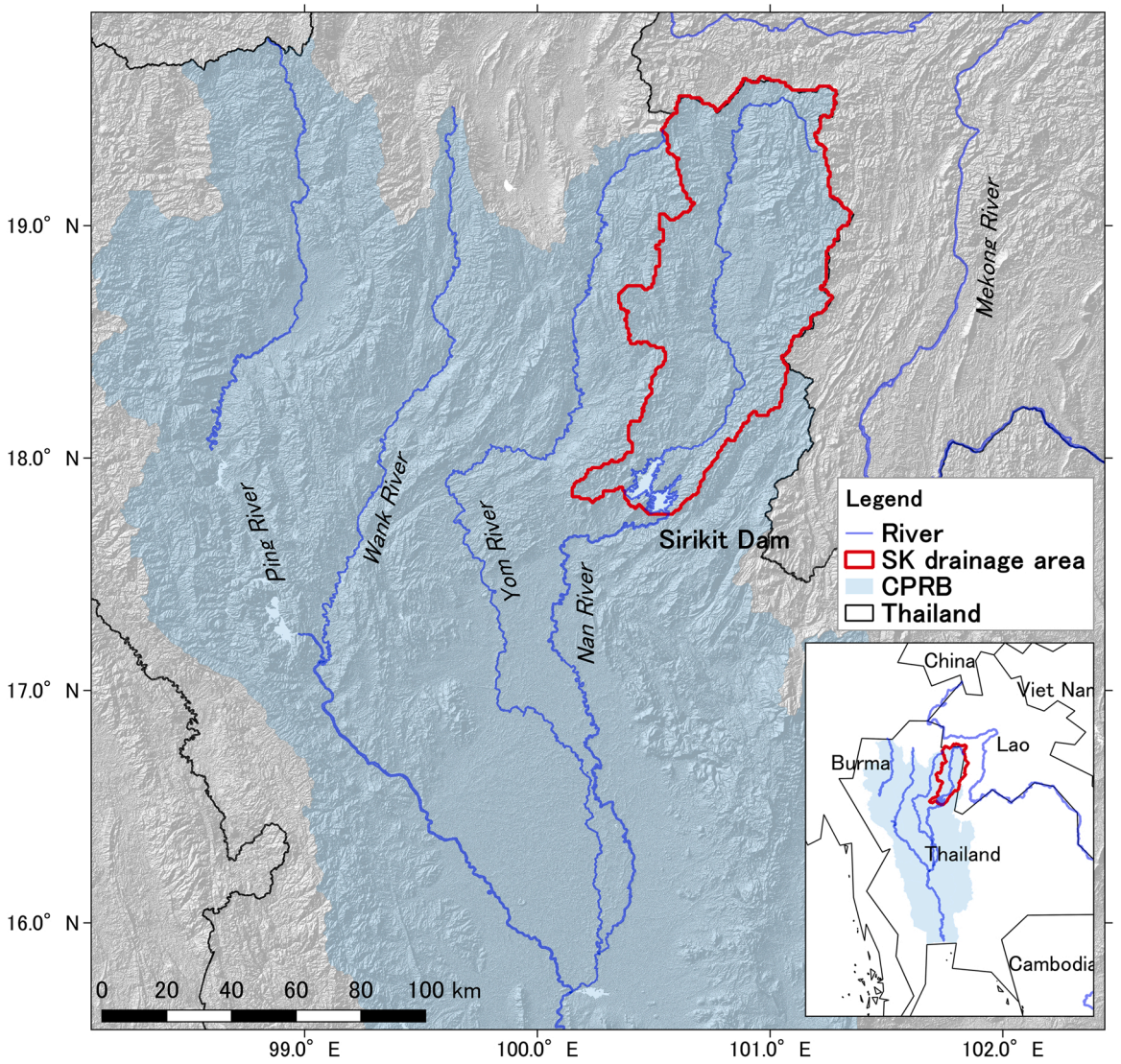

Fig. 1. Location of study basin and the Sirikit Reservoir (SK).

(2001) demonstrated that using ESP forecasts in a real-time DP reservoir system optimization model provides more efficient operating decisions than employing historical time series. Kim et al. (2007) reported that updating operation policy using ESP forecasts with DP is appropriate for the Geum River multi-reservoir system in Korea. In addition, operational ensemble hydrometeorological predictions have been used with a hydrological model to predict a reservoir inflow and adapted it to real-time reservoir optimization using DP for water use in a drought event (Nohara and Hori, 2018). The study reported that this approach generally mitigates drought damage compared with considering historical flow time series. Although these studies indicated that association of ensemble forecast information with DP for reservoir optimization can improve the operation efficiency, information regarding the methods for performing reservoir inflow forecasts using ensemble hydrometeorological predictions with hydrological model (reservoir inflow prediction approach) such as real-time state update produce is scarce. This procedure becomes more important for a reservoir located in a tropical-climate basin with distinct wet and dry hydrological conditions, such as the CPRB.

Recently, the CPRB frequently faces drought conditions since 2011 massive flooding occurred in the basin. The accumulated annual inflow of two major dams–Bhumibol and Sirikit–during 2012–2019 is 17.1% lower than the historical 30-year average, which means 6 in 8 years of annual inflow are lower than the historical mean. Especially the severe drought in 2015 and 2019, the accumulated annual inflow of two dams is 48.5% and 40.0% lower than the historical mean, respectively. Regarding the downstream water requirement, this resulted in a low storage volume of the reservoirs as a result of the imbalance between inflows and outflows. The events resulted in difficulties in water management for the coming years as a result of insufficient reservoir water storage. In Thailand, the drought problem over the long-term develops into a primary social and economic issue (Zenkoji et al., 2019).

Therefore, this study aims to introduce the forecast information for water resources management to mitigate the impact of drought. The main objectives are as follows: (1) to investigate the ability of river flows forecasting using a distributed hydrological model with ensemble precipitation forecasts (EPF), and (2) to utilize the river flow prediction for real-time reservoir optimization using DP to mitigate the drought event for a case study in 2019. For this purpose, a physically-based distributed hydrological model is adopted. An adaptive mode of operation (state variable update) with different update procedures to assess the effect of the model's initial state condition is also utilized on the results of river flow forecasts. Medium-range EPFs are used to determine the reservoir inflow 2 weeks in advance of reservoir inflow forecast. Then, the optimization of reservoir release is examined in different scenarios of optimization using the 2-week inflow forecasts. In Section 2, a case study of the difficulties for reservoir operation of the Sirikit Dam during the drought event in 2019 has been proposed. In Section 3, the hydrological model is calibrated and validated in offline mode prior to its application and its use for forecasting. In Section 4, the methodology of implementing the real-time inflow forecast using ensemble precipitation forecasts is described, and the effect of the model's initial conditions with different model state update procedures on the inflow forecast results is evaluated. In Section 5, real-time reservoir optimization for 1-week advanced release strategy using forecast inflows is examined with different scenarios regarding future long-term inflow assumptions. In Section 6, the advantages of

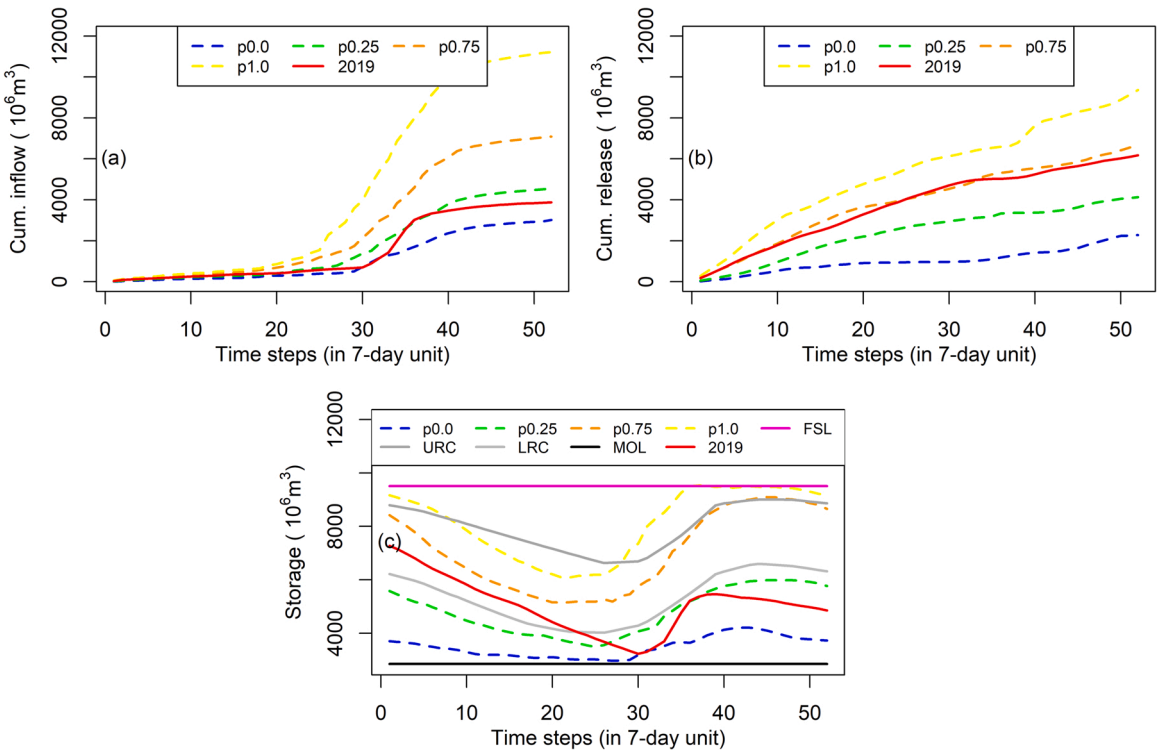

Fig. 2. Operation record of Sirikit Reservoir in 2019 (a) reservoir inflow compared to historical record (b) release compared to the historical record and (c) reservoir storage (p0.0 is minimum, p0.25 is 25th percentile, p0.75 is 75th percentile and p1.0 is maximum).

introducing ensemble hydrometeorological forecasts are demonstrated for real-time optimization of Sirikit reservoir operation during 2019.

2. Current dam operation at the Sirikit dam

The Sirikit Dam contains 6660 million m^3 of effective storage and 500 MW of power generation capacity located on the Nan River, one of the four main tributaries of the Chao Phraya River. The dam controls 13,130 km^2 of drainage area. The main functions of the dam include irrigation purposes, domestic and industrial use, flood control, ecological conservation, and power generation (Amnatsan et al., 2018). The location of the study basin is shown in Fig. 1.

Fig. 2 shows the operation records of the Sirikit reservoir during 2019 compared to the 30 years historical data in the percentile of each 7 days unit. Fig. 2a and b show the comparison of accumulated reservoir inflow and release, respectively. Fig. 2c show the comparison of reservoir storage between 2019 and historical data. Due to unpredicted inflow, reservoir operation faces significant challenges in controlling water for society. The reservoir storage level was higher than the lower rule curve (LRC) at the beginning of the year (see Fig. 2c), whereas the released volume is relatively high (close to the 75th percentile) because of the downstream demand and power supply requirement during the dry season, as shown in Fig. 2b. However, the low inflow volume from the beginning to the middle of the wet season was unexpected. Compared to the 30 years historical data, the reservoir inflow volume is low (lower than the 25th percentile), as shown in Fig. 2a. This event presented difficulties for reservoir operation and resulted in a low storage level (lower than LRC) after mid-August and led to a low level of reservoir storage at the end of the year (significantly less than the LRC), as shown in Fig. 2c.

For effective basin water management, reservoir operation requires forecasting information. The dam reservoir water level in 2019 is historically low and to investigate the precipitation forecast to reduce the drought disaster is an urgent issue. Therefore, we selected this period as a case study to evaluate the performance of release strategy estimation forecasting 1-week in advance using medium-range weather forecast information and the reservoir optimization process.

3. Reservoir inflow prediction model

The 1K-DHM is a distributed hydrological model based on kinematic wave flow approximation that considers surface–subsurface flow. The elevation and flow direction are determined using topographical data provided by HydroSHEDS (Lehner et al., 2006) in digital elevation models with a resolution of 30 s (approximately 1 km). Each cell of the hydrological process consists of river and slope flow components (Tanaka and Tachikawa, 2015). Meema and Tachikawa (2020) incorporated unconfined bedrock aquifers into the slope flow component of the original model to improve the long-term river flow simulation in a tropical-climate basin and this improved model was used as an inflow. The continuity and momentum equations for the surface soil layer are as follows:

$$\frac{\partial h_s}{\partial t}+\frac{\partial q_s}{\partial x}=r-e-p_u \tag{1}$$

$$q_s(h_s)=\begin{cases} \&d_m k_m\left(\dfrac{h_s}{d_m}\right)^{\beta} i \quad (0\le h_s\le d_m) \\ \&d_m k_m i+(h_s-d_m)k_a i \quad (d_m\le h_s\le d_a) \\ \&d_m k_m i+(h_s-d_m)k_a i+\dfrac{\sqrt{i}}{n_s} \quad (h_s-d_a)^m (d_a\le h_s) \end{cases} \tag{2}$$

where q_s is the runoff per unit slope width, h_s is the water depth, r is the rainfall intensity, e is the evapotranspiration, p_u is the vertical infiltration rate from the surface soil layer into the bedrock aquifer, d_m is the maximum water content in the capillary pore, k_m is the hydraulic conductivity when the capillary pore is saturated, β is an exponent parameter that describes the relationship between hydraulic conductivity and water content, d_a is the maximum water content in the effective porosity, k_a is the saturated hydraulic conductivity, n_s is the Manning's roughness coefficient for surface flow, i is the slope gradient, and $m = 5/3$.

The continuity and momentum equations for bedrock aquifer layer are as follows:

$$\frac{\partial h_u}{\partial t}+\frac{\partial q_u}{\partial x}=p_u \tag{3}$$

$$q_u(h_u)=\alpha_u {h_u}^2 \tag{4}$$

where d_u is the total effective depth of rock fracture in the unconfined bedrock aquifer, h_u is the total water depth in the fracture of the aquifer, and $\alpha_u = k_u i/d_u$, where k_u is the hydraulic conductivity that corresponds to the actual cross-sectional area of flow in the rock fracture, and i is the gradient of the hillslope.

The discharge from the slope flow component on both sides of the river channel contributes to the river channel component as the lateral discharge per unit length. The discharge from the upper cells is assigned to the river channel component of the cell as the boundary condition. The river flow of the river channel component is computed by the following 1D kinematic wave equations:

$$Q = \alpha A^m \tag{5}$$

$$\frac{\partial A}{\partial t} + \frac{\partial Q}{\partial x} = 2(q_s + q_u) \tag{6}$$

where Q is the river discharge, A is the cross-sectional area, $m = 5/3$ and $\alpha = \sqrt{i}/(nB)^{2/3}$ in which the river channel (B) is assumed to be a wide rectangle and vary each grid based on the grid drainage area determined by $B = aA_{grid}{}^b$ (where A_{grid} is grid drainage area, a and b are constant parameters).

The model was calibrated and validated before applying it to the inflow forecast. To apply the model for long-term forecasting, the calibration periods was set to contain the seasonal hydrological characteristics of the basin (wet and dry seasons). The SCE-UA algorithm (Duan et al., 1994) was applied to optimize the model parameters by searching for the parameter with the smallest root mean square error (RMSE) when compared with observations. Designing the range of the parameters is important to identify the parameter set. The model calibration method was described by Meema and Tachikawa (2020). To determine the parameter of the total effective depth of rock fracture (d_u) for the study basin, the hydrogeological map of the study basin was used and resulted in most of the area is shale. Considering the porosity of 0.0−0.1 (Freeze and Cherry, 1979), the total storage of bedrock aquifer may be ranged from 0.0 to 3.0 m.

The inflow of the Sirikit reservoir in 2014, which is considered a normal hydrological year, was selected as the calibration period. The optimized model parameters are listed in Table 1. The optimal parameter such as the total effective depth of rock fracture (d_u) agreed with the hydrogeological map which the aquifer productivity is quite small. This indicates that the effective depth may be much smaller than the maximum of the designed range. The same parameter set was applied to the validation periods in 2008 and 1998, which were considered wet and dry, respectively.

The model performed well in both calibration and validation periods with an RMSE less than 63.9 million m^3 (1.1% relative difference using mean annual inflow) and Nash–Sutcliffe efficiency (NSE) coefficient greater than 0.82, as shown in the comparison between simulated and observed inflow of the reservoir in Fig. 3. The model efficiently represents the inflow characteristics of the basin for both the wet and dry seasons for all simulation periods. This model, with the optimized parameter set, was applied to produce real-time inflow forecasts for the 2019 Sirikit reservoir.

4. Ensemble inflow prediction using European Centre for Medium Range Weather Forecasts (ECMWF) precipitation forecast

4.1. Ensemble Precipitation Forecast used in the study

TIGGE (THORPEX Interactive Grand Global Ensemble) is a database of ensemble medium-range forecasts conducted by different forecasting centers worldwide for conducting scientific research (Bougeault et al., 2010). Ensemble Prediction System data are available from approximately ten of these forecasting centers.

Among all data on TIGGE, ECMWF has advantages in a number of forecast members (associated with high forecast uncertainty) and spatial resolution (applicable for the study basin) compared to other forecasting systems. Regarding these advantages, it was selected as the EPF data for generating reservoir inflow forecasts in this study. The ECMWF forecasts consist of 51 members of precipitation with approximately 0.5° resolution for the whole globe. Initial uncertainties are considered using a singular vector technique. A stochastic scheme is used to model uncertainties resulting in possible variations in physical parameterizations (Buizza et al., 2007). The data are available twice a day at 00:00 UTC and 12:00 UTC with time steps of 6 h and 15 d of forecast lead time.

4.2. Real-time state update of hydrological model

The update procedure of the model state variables is based on observed errors in river flow, and empirical methods or Kalman filtering has been used (Moore et al., 2005; Romanowicz et al., 2006). Using Kalman filtering with complex distributed and nonlinear models results in highly complex computations (O'Connell and Clarke, 1981). A cost-effective approach has been developed for computation using an empirical data assimilation procedure and applied to a large-scale hydrological model (Collischonn et al., 2005).

Therefore, we adopted this empirical data assimilation procedure to incorporate the large-scale distributed hydrological model (as

Table 1
Optimized parameters of the hydrologic model.

Parameter	Units	Value
n_s	$m^{-1/3}/s$	0.975
k_a	m/s	1.14×10^{-4}
d_a	m	3.179
d_m	m	2.984
β	–	19.906
k_u	m/s	8.46×10^{-5}
d_u	m	0.323
k_v	m/s	1.08×10^{-7}

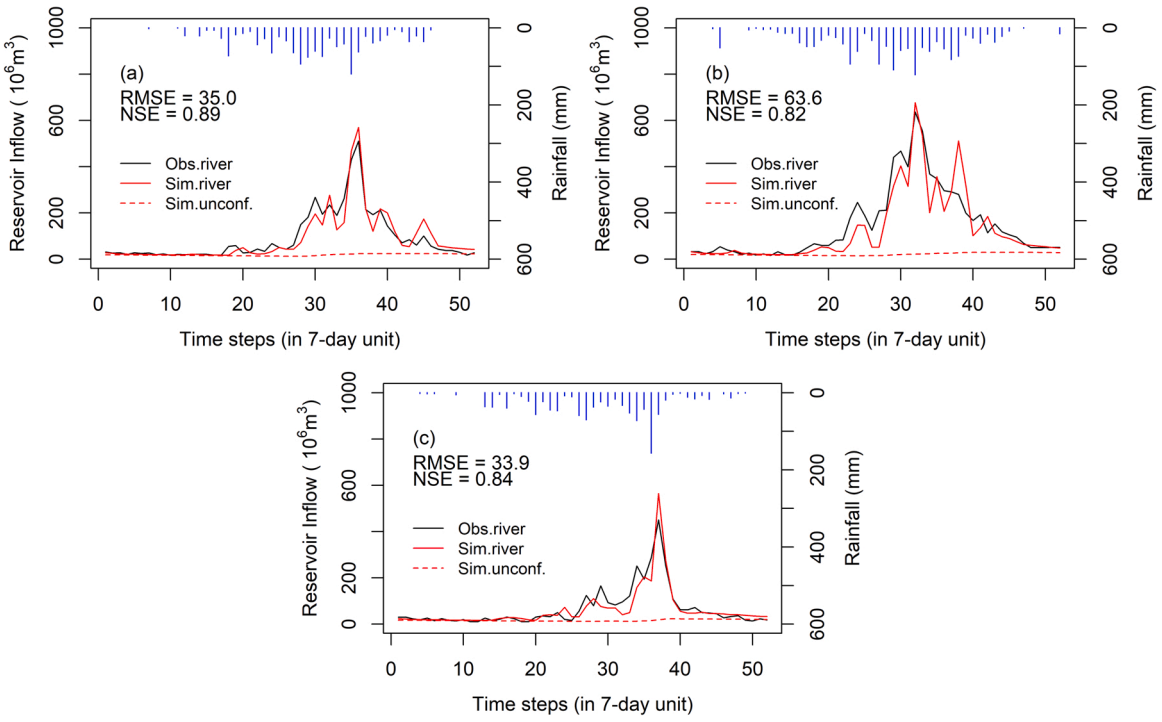

Fig. 3. Comparison between simulated and observed inflow at the Sirikit dam (a) during the calibration period (b) validation period 1 (c) validation period 2 (RMSE [million m^3] and NSE [-]).

explained in Section 3) to obtain the initial state of the basin (at *t*0) using observed and ensemble precipitation forecasts as the model input prior to performing reservoir inflow forecasts. The updating correction factor (*FCA*) is calculated at gauge station *k* using the following equation:

$$FCA_k = \frac{Q_{obs,\ k}}{Q_{cal,\ k}} \tag{7}$$

where $Q_{obs,\ k}$ and $Q_{cal,\ k}$ are the observed and calculated river discharges at gauge station *k*.

To evaluate the updating procedure during the initial analysis period, different empirical equations were investigated in this study. First (model states update type 1), the correction factor is directly applied to update the state variables for any cell *i* located upstream of gauge station *k* as expressed in Eq. (8). Second (model states update type 2), the correction factor is applied to correct the state variables for any cell *i* located upstream of gauge station *k* considering a drainage area factor of the upstream grids at each cell, as expressed in Eq. (9).

$$S_{up,\ \ i,k} = FCA_k \bullet \mathrm{S}_{\mathrm{cal,\ \ i}} \tag{8}$$

$$S_{up,\ \ i,k} = FCA_k \bullet \mathrm{S}_{\mathrm{cal,\ \ i}} \bullet \left(\frac{\mathrm{A_i}}{\mathrm{A_k}}\right) + \mathrm{S}_{\mathrm{cal,\ \ i}} \bullet \left(1 - \frac{\mathrm{A_i}}{\mathrm{A_k}}\right) \tag{9}$$

where $S_{up,\ i,\ k}$ are the updated model state variables at cell *i* located upstream of gauge station *k*, $S_{up,\ i,\ k}$ can be substitute with the variables of the hydrological model such as river discharge (*Q*), lateral discharge from the surface soil layer (q_s), and the bedrock aquifer layer (q_u); A_i and A_k are the drainage areas upstream of cell *i* and gauging station *k*.

4.3. Real-time reservoir inflow forecast algorithm

Fig. 4 illustrates the procedure of the reservoir inflow forecast using the EPF. The simulation can be divided into two periods: the initial analysis and forecast periods. For real-time forecasting, it is necessary to operate the model in adaptive mode (Moore et al., 2005) for which the model output is based on previous model inputs as well as previously observed information that is used to update the model prior to a new forecast. Thus, this study proposes an initial analysis period to account for uncertainties in the model initial conditions before the forecast period is performed. For this purpose, data assimilation (as explained in Section 4.2) is adopted to improve the estimate of the initial states of the model and to reduce the simulation errors in the forecast period (Madsen and Skotner, 2005).

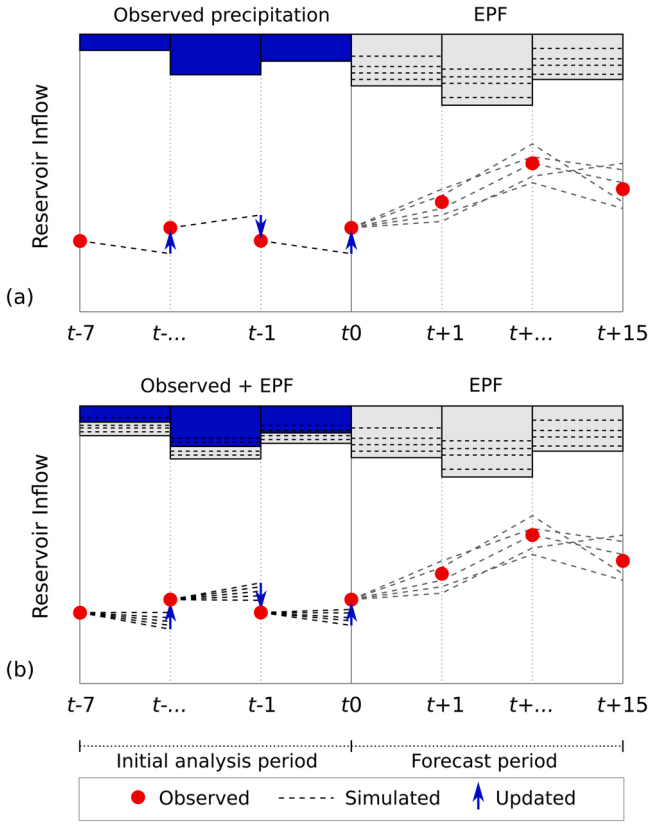

Fig. 4. Schematic of inflow forecast procedure using (a) observed rainfall and (b) a combination between observed and end ensemble forecasts up to the starting time of the forecasts ($t0$), and ensemble precipitation forecast up to the lead time.

We not only considered model state variables for the data assimilation implementation, but also the errors due to model input. To assess the errors due to input data during the initial analysis period, two procedures of input precipitation data for the model were considered. First, a single pattern of observed data was applied to the model. Second, a combination of observed data and ensemble forecasts with 52 patterns (one pattern of observation + 51 patterns of ensemble forecasts) of precipitation was applied to the model. Fig. 4a describes the procedure of using observed precipitation and model state updates up to the starting time of the forecasts ($t0$). Then, the EPFs were applied to the model as forcing input data up to the lead time ($t + 15$) for the 15-d reservoir inflow forecasts. Fig. 4b describes the procedure of using a combination of observed and ensemble forecast data and the update procedure of the model states up to the starting time of the forecasts ($t0$). Using 52 precipitation patterns during the initial analysis period, 52 flow patterns were obtained. To select the flow pattern that represents the model states at the starting time of the forecasts ($t0$), the highest NSE coefficient computed from the comparison between each simulated flow pattern with the observation during the initial analysis period was selected.

Data assimilation methods used during the initial analysis period to reproduce the initial state of the model at the initial time of the forecast ($t0$) are summarized in Table 2. The model state variables were updated in forecast methods 1 and 2 using Eq. (8) and in forecast methods 3 and 4 using Eq. (9). A single pattern of observed precipitation was used in forecast methods 1 and 3 (Fig. 4a). For forecast methods 2 and 4, 52 precipitation patterns were used (Fig. 4b). For the forecast period (all methods), precipitation forecasts were used, and the observed precipitation was applied in this study to evaluate the inflow forecast procedures as a possibly perfect forecast of precipitation.

Table 2
Description of data assimilation methods used in the initial analysis period and input forcing data for each simulation period.

Method	Initial analysis period (t-7 − $t0$)			Forecast period ($t0$ − t + 15)	
	State update type	Input data	No. input pattern	Input data	No. input pattern
1	1	Obs.	1	Obs. + Ens. Forecast	52
2	1	Obs. + Ens. Forecast	52		
3	2	Obs.	1		
4	2	Obs. + Ens. Forecast	52		

5. Reservoir optimization with ensemble inflow forecast in Sirikit Dam

5.1. Application of DP for reservoir optimization

To interpret the results of the ensemble inflow forecast, the general method is to consider the mean value (ensemble mean) or median, which represents the tendency of all ensemble forecast members. To optimize the operation strategy of the reservoir using the ensemble mean or median of the ensemble inflow forecast, the deterministic DP (DDP) can be applied (Nohara and Hori, 2018).

By using DDP in reservoir problems, the reservoir storage at time t is divided into decision-making stages (S_t). The optimized water release (R_t) at each state is selected based on the minimum value of the sum of the current drought damage ($B_t(R_t)$) and future drought damage function ($F_{t+1}(S_{t+1})$). The computation is started at the end of the optimization time (the final stage) and then moved backward to the beginning stage (Louoks and Falkson, 1970). The recursive equation for optimization can be defined by the following equation:

$$F_t(S_t) = \min_{[f_0]}[H_t(R_t) + F_{t+1}(S_{t+1})] \tag{10}$$

where t is the time period, and $H_t(\cdot)$ is the drought damage function of period t and $F_{t+1}(S_{t+1})$ is the future drought function which represents the minimal drought damage expected after time step t when the storage state is S_t at time step t.

5.2. Implementation with the optimized strategy and scenarios

We assume that the simulation for 1-week in advance released strategy performs every Sunday. The volume of water released from the reservoir follows the simulated strategy throughout the week. A total of 52 weeks in 2019 was the target period of this study.

Fig. 5 presents the optimization scheme for a target week (t) release strategy using DP. To adopt DP, the penalties must be utilized at lower reservoir storage levels after the final time step of optimization. This is to ensure that the reservoir will not draw down to low storage levels by releasing excess water to generate quantified benefits during the optimized period. For this purpose, the sum of future benefits was applied to each storage level after the final time step of the optimization (F_{t+2}) as losses or penalties.

To calculate penalties at the stage of $t + 2$ (F_{t+2}) for each storage level, the next year's benefits (possible future benefit in 2020) were also considered. However, to begin the calculation of the DP recursive equation, as expressed in Eq. (10), the initial assumption is that all future benefits (losses or penalties) will be zero at some point of time (Loucks et al., 2005). For this purpose, a dummy year was proposed to quantify the benefits or penalties at the end of 2020 ($F_{T''+1}$), avoiding the assumption of terminating operation. The 50th percentile of the 30-year historical data was used for the reservoir inflow in the dummy year. Thus, all future benefits (losses or penalties) after the final stage of the dummy year (F_{T^*+1}) were defined as 0. Following Eq. (10), we can start calculating the penalties (F) in each stage progressing backward to the stage after the optimization period ($t + 2$). Finally, the penalties at the stage after the optimization period (F_{t+2}) for each storage level were obtained.

According to the limitation of forecast information (approximately 2 weeks), the future long-term reservoir inflow that is used to calculate the penalties after the optimization period ($t + 2$) was proposed with different assumptions, which is summarized in Table 3. The general method for future inflow assumptions is to use the 50th percentile of historical data for all remaining periods (up to the end of 2020). This is proposed in Scenario 1. The 25th percentile of historical data was adopted in Scenario 2, assuming drought conditions.

To assess the effect of the future inflow assumption, it was assumed that the assumption is perfect, as proposed in Scenario 3. A combination of perfect forecasting and future assumptions was proposed in Scenario 4. To assess the effect of the use of forecast inflow in optimization, Scenario 5 was introduced with the general procedure using the 50th percentile of historical data as the future inflow assumption.

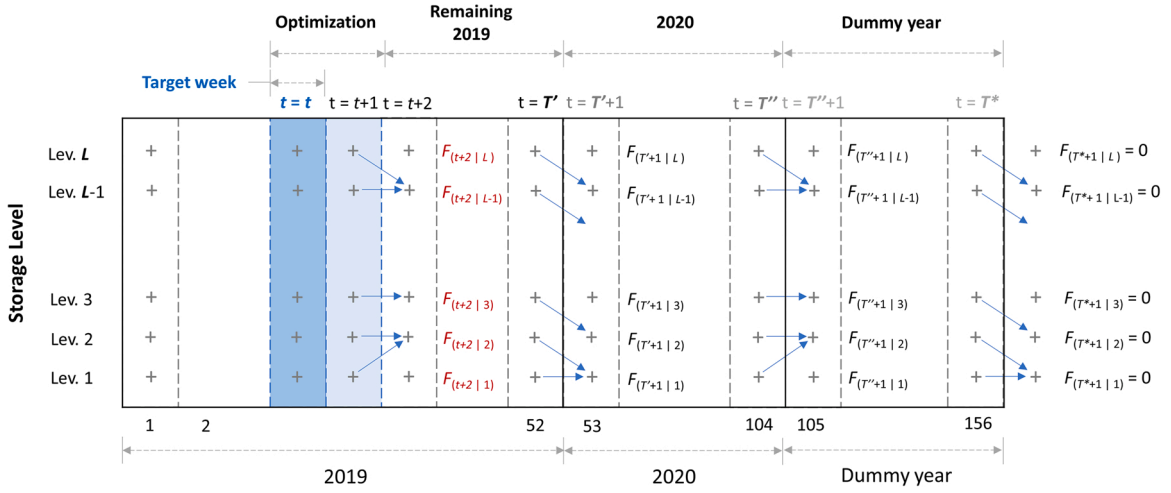

Fig. 5. Optimization scheme for any target week release strategy (R_t) and calculation of ending storage penalties ($F_{(t+2)}$) using DP.

Table 3
Description of optimization scenarios with different future long-term inflow assumptions for each period. (Hist. is historical data, p50 and p25 are 50th and 25th percentile respectively).

Scenarios	Periods			
	Optimization	Remaining 2019	2020	Dummy
Scenario 0	Baseline scenario (actual operation)			
Scenario 1	Forecast mean	Hist. p50	Hist. p50	Hist. p50
Scenario 2	Forecast mean	Hist. p25	Hist. p25	
Scenario 3	Forecast mean	2019	2020	
Scenario 4	2019	2019	2020	
Scenario 5	Hist. p50			

The 1-week advanced release strategy (R_t) obtained from the optimized process can be implemented for any initial reservoir storage level (S_t) at the target time (t). This signifies that this strategy can be implemented under different flow patterns using linear interpolation among the release tables obtained from the optimization process.

To determine the strategy performance, the strategies were utilized on observed flow patterns (using a forward calculation). The strategy performance is evaluated based on the sum of the drought damage function from the present to the future. Storage of the target time (S_{t+1}) can be estimated using the continuity equation of the reservoir routing, which will be the initial storage of the following time step. The same procedure will be repeated with the next operation strategy.

5.3. Objective function

The objective function for the reservoir operation optimization in the drought problem may be defined as a minimization of the total drought damage over the study period. The objective function for this problem is expressed as follows:

$$min \sum_{t=1}^{T} H_t \tag{11}$$

where T is the number of optimization stages, and H_t is the drought damage function at stage t. A drought damage function proposed by Ikebuchi et al. (1990) was employed in this case study for the objective function of optimization. The function is defined by the following equation:

$$H_t(R_t) = \frac{[max(D_t - R_t, 0)]^2}{D_t} \tag{12}$$

Where D_t is water demand required from the reservoir. This function represented the absolute value of the water gap multiplied by the rate of the gap to the demand, giving equal weight to both the absolute value and the rate of the gap when the drought damage is evaluated.

Water demand from the Sirikit reservoir generally depends on the correlation between irrigation demand and hydropower generation as well as the amount of water supply from other sources (such as release from the Bhumibol reservoir and side flows from other tributaries. For this purpose, huge information is required leading to the huge dimension of analysis. To simplify this, the amount of historical release from the reservoir might specify as the target for the water requirement from the reservoir. This assumption is based

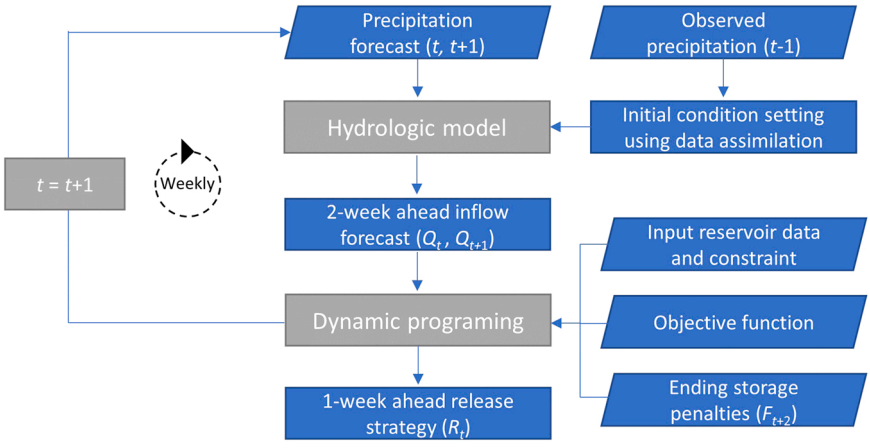

Fig. 6. Optimization of dam release strategy for long-term reservoir operation using EPF.

on the assumption that a particular amount of water is released from the Sirikit reservoir supplying the existing demand in the CPRB.

Water allocation from the reservoir to irrigation sector in Thailand varies annually (Takeda et al., 2016). Regarding the drought condition in 2019, the downstream water requirement such as from the irrigation sector may require more water from the reservoir than usual. Thus, we assumed that the actual release during 2019 could supply the downstream demand. For the future assumption demand (for calculating future drought damage), the downstream water demand may consider as the usual. Thus, the average releases during 2004−2018 (except the unusual release in 2011) from the reservoir was used.

5.4. Optimization framework for dam release strategy using DP

The objective of this study is to develop a future release strategy for large-scale reservoirs using weather forecasts. For this purpose, the optimization process of the released strategy for long-term reservoir operation using EPF is illustrated in Fig. 6.

For real-time river flow forecasting, an initial condition setting of the hydrological model is necessary. The previous week's (t-1) flow condition (initial analysis period) was simulated with observed rainfall (forecast method 3 was selected, discussed in Section 6.2) to determine initial condition of the model using adaptive mode (data assimilation is associated). The model state variables at the beginning of the forecast period obtained from the simulation in the initial analysis period (t-1) were assigned to the model as the initial state condition (see Section 4).

The 2-week inflow forecast (Q_t and Q_{t+1}) obtained from the hydrological model (simulated with 2-week advanced EPF) was input into the DP to optimize the 1-week advanced release strategy (R_t) at any storage level. To optimize the release strategy, the future benefit at the end of the target period (F_{t+2}) is required to associate the penalties to lower storage levels of the reservoir (see Section 5.2). Objective function of the drought damage is required for the optimization process (see Section 5.3). Reservoir information such as elevation-storage-area, maximum–minimum storage, evaporation rate from the water body at any stage, and generated power capacity are required. Furthermore, the minimum and maximum released capacities are assigned to the DP algorithm as the constraint for the reservoir release condition. For the reservoir release constraint in this study, two release functions were adopted for DP. Firstly, the maximum total release (turbine release and spillway release) was used for unusual release such as flood events considering the capacity of the downstream river channel. Secondly, the constraint for usual release (power generation and downstream water requirement) regards the historical maximum and minimum demands varying monthly.

6. Results and discussion

6.1. Performance of EPF

Fig. 7a and b present the comparison of accumulated basin-averaged precipitation between forecasts and observations for accumulated 1 week (days 1–7) and accumulated 2 weeks (days 1–14), respectively. The forecast is capable of estimating precipitation during the dry season (around weeks 1–17 and weeks 45–52). However, during the wet season, there are some differences between precipitation forecasts and observation, especially during the start to mid of the wet season (around weeks 18–29), which resulted in an overestimation of the accumulated precipitation for both 1 week and 2 weeks.

In contrast, using the mean of forecast ensembles for accumulated basin precipitation, the forecast performed well, when compared

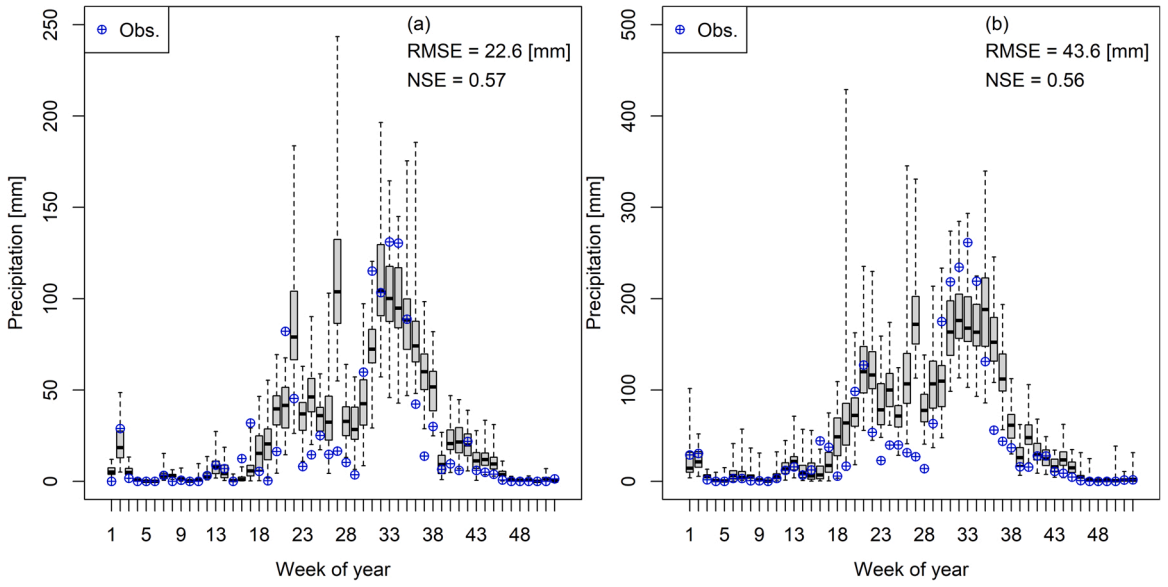

Fig. 7. Comparison of accumulated basin-averaged precipitation between observed and forecasts (a) 1 week of forecast (b) 2 weeks of forecast.

to the observation, with an RMSE value of 22.6 mm (2.0% relative difference using annual precipitation) and 43.6 mm (3.9% relative difference using annual precipitation) for 1 week and 2 weeks, respectively.

6.2. *Performance of inflow forecasting*

Figs. 8 and 9 present the reservoir inflow comparison between forecasts (box plot) and observations in different forecast methods for 1 and 2 weeks accumulated inflows, respectively. Precipitation forecasts were used during the forecast period, and the observed precipitation was adopted to evaluate the forecast procedure as a possible perfect forecast. The performances of inflow forecasts such as RMSE and NSE in different forecast methods were calculated by comparing the mean of the forecast ensembles with the observations, as summarized in Table 4.

According to the results obtained from different forecast methods, the model initial state condition (including its spatial distribution) has a primary effect on inflow forecasts. This results in a significant difference in the forecast inflow volume. Using the state update a type 1 scenario (applied same ratio to all upstream grids), the forecast inflow had a significant fluctuation among the forecast members compared to using the state update type 2. The use of forecast and observed precipitation resulted in a significant difference in the forecast volume, especially during high flow (see Fig. 8a, b, a, and b). Moreover, the 2-week accumulated inflow forecast resulted in a significant overestimation throughout the year compared to the observations (see Fig. 9a and b).

Using the state update type 2 (considered grid drainage area), the inflow forecast had more stable results among the members compared to the results obtained from the type 1 state update. There is no primary difference in the simulated results obtained using forecasts and observed precipitation (see Fig. 8c, d, c, and d). Furthermore, the accumulated forecast inflow for 1 and 2 weeks corresponded well with observations.

This may be described by comparing the spatial distribution of the model's initial state (the model state at the initial forecast time, *t*0) that resulted in a difference in the forecast inflow. For example, Fig. 10 presents a comparison of the initial model state spatial

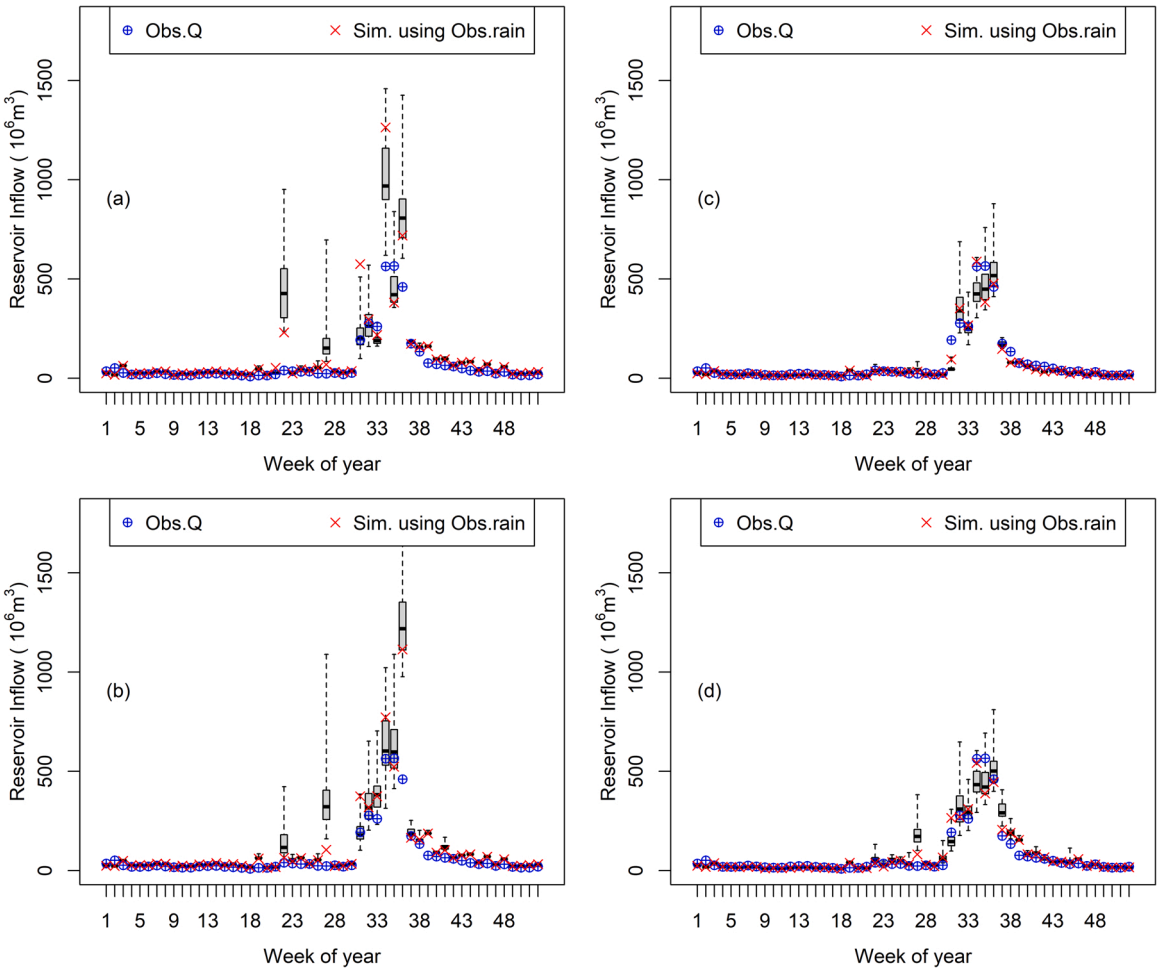

Fig. 8. Comparison of accumulated 1 week reservoir inflow between forecasts (box plot) and observation in different forecast methods (a) method 1 (b) method 2 (c) method 3 and (d) method 4.

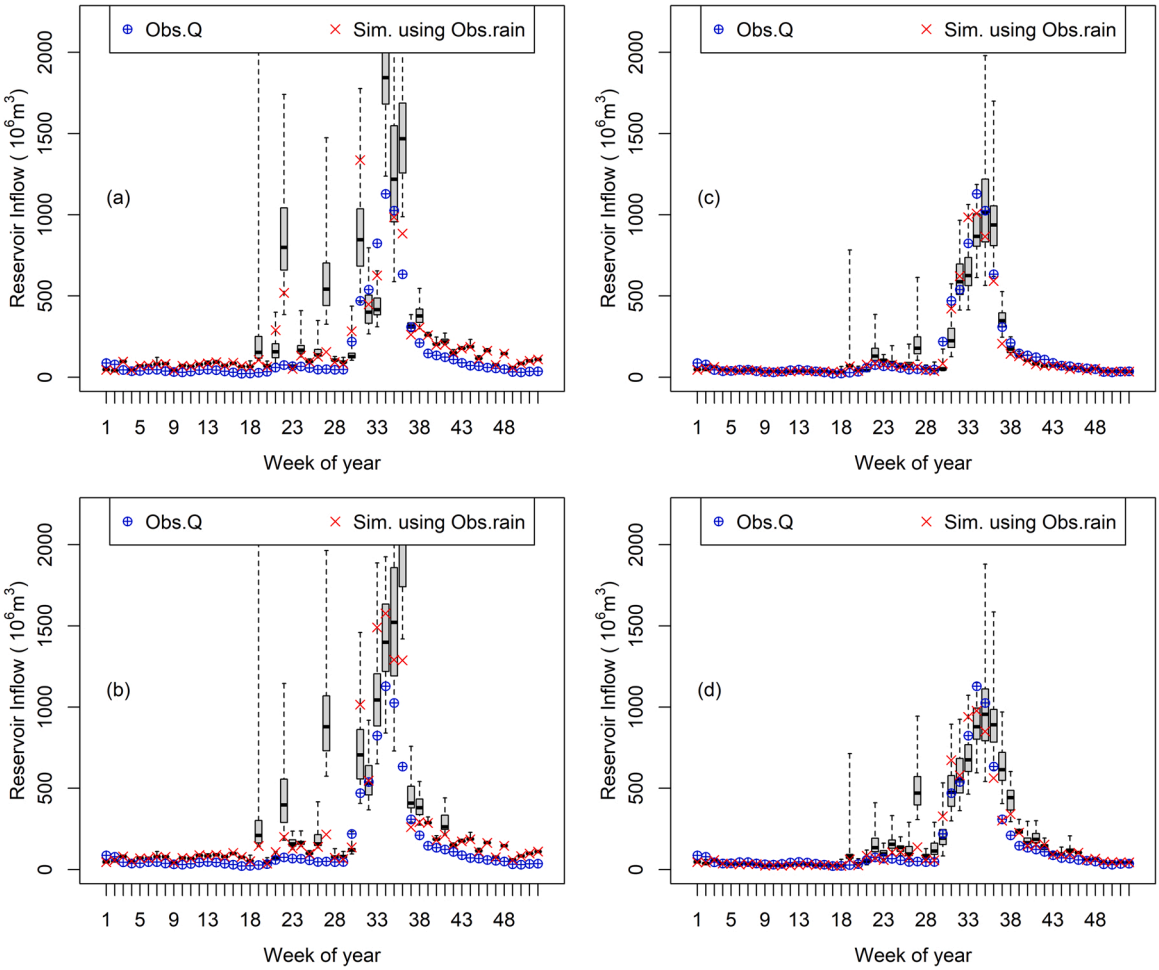

Fig. 9. Comparison of accumulated 2 weeks reservoir inflow between forecasts (box plot) and observation in different forecast methods (a) method 1 (b) method 2 (c) method 3 and (d) method 4.

Table 4
Performance of inflow forecasts in different forecast methods and input forcing data (RMSE [million m3] and NSE [-]).

Method	One-week				Two-week			
	Forecasts		Observation		Forecasts		Observation	
	RMSE	NSE	RMSE	NSE	RMSE	NSE	RMSE	NSE
1	104.2	0.32	124.0	0.04	236.5	0.07	208.4	0.28
2	126.6	0.004	103.3	0.34	270.5	–	178.2	0.47
3	36.1	0.92	33.2	0.93	78.7	0.90	48.5	0.96
4	43.5	0.88	33.7	0.93	105.9	0.81	58.4	0.94

distribution for week 31 (July 28, 2019, 00:00 UTC) using different forecast methods. Fig. 10a–d present the distributed grid discharge ranged from 0.0 to 265.0 m^3/s that emphasize the discharge state in the mainstream. Fig. 10e–h present the distributed grid discharge ranged from 0.0 to 1.0 m^3/s that emphasize the discharge state for the most of catchment area (small streams). The spatial distribution of discharge state at the upstream grids shows a difference in value compared among different update methods (see the procedure in Section 4) in contrast to the river discharge at the basin outlet (observed station) having the same value for all methods. Fig. 10a, b, e and f present the spatial distribution of the initial model state resulting from update procedure type 1 that the correction factor (*FCA*) is directly applied to update the state variables for any upstream grid of the observed station as expressed in Eq. (8), which exhibited greater river discharge at the upstream grids than Fig. 10c, d, g and h resulting from update type 2 that the correction factor (*FCA*) is reduced when updating the state variables for any upstream grid based on a drainage area factor at each cell (the ratio of drainage area between any upstream grid and the observed station) as expressed in Eq. (9).

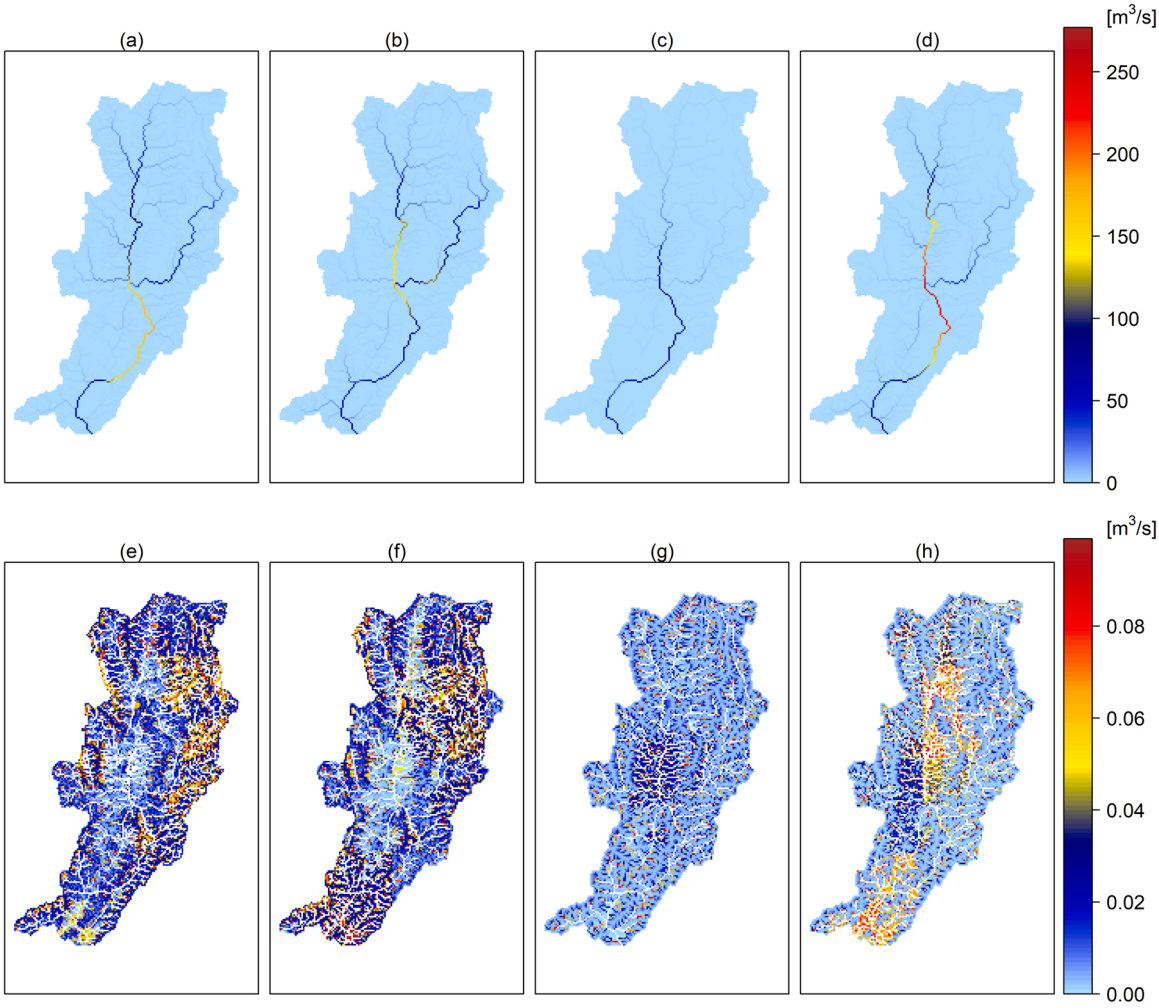

Fig. 10. Comparison of initial state conditions for the simulation of week 31 among different forecast methods (a) method 1 (b) method 2 (c) method 3 and (d) method 4 which value range from 0.0 to 265.0 m^3/s, (e) method 1 (f) method 2 (g) method 3 and (h) method 4 which value range from 0.0 to 1.0 m^3/s.

The difference in the initial state value resulted in different inflow forecasts, as shown in Fig. 11. The forecast hydrograph in Fig. 11a and b resulting from state updated type 1 presented a higher forecast inflow than those (Fig. 11c and d) from state updated type 2. Higher discharge from the upstream grids at the initial state of forecast simulation resulted from the higher update coefficient flow to the outlet, when the simulation time was extended.

There is no primary difference in the forecast results compared to the use of different forcing data during the initial analysis period. Using only observed precipitation during the initial analysis period, the inflow forecast resulted in higher performance and lower simulation cost. Therefore, it may be considered as a cost-effective procedure for setting the initial states of the model prior to performing the forecast. As forecast method 3 resulted in satisfactory performance and reduced simulation cost, the result from this method was adopted to optimize the Sirikit Dam release strategy.

6.3. Reservoir optimization results

Fig. 12 presents the results of the reservoir operation by adopting the release strategies obtained from different scenarios of the real-time optimization process. Fig. 12a shows a comparison of the reservoir releases in different optimization scenarios. The actual release (Scenario 0) is significantly larger than the average historical release during May – July (week 18−30) increased demand for downstream water use due to the unexpected drought period. Although the reservoir storage might be considered to be at a high level (much higher than the LRC), the storage gradually decreased to low storage levels as a result of the imbalance between reservoir inflows and outflows. The water release hydrographs resulting from the optimization process (scenarios 1−5) have a similar tendency to reduce water releases smaller than the actual operation (Scenario 0) to mitigate the drought damage in the future based on different scenarios of optimization criteria.

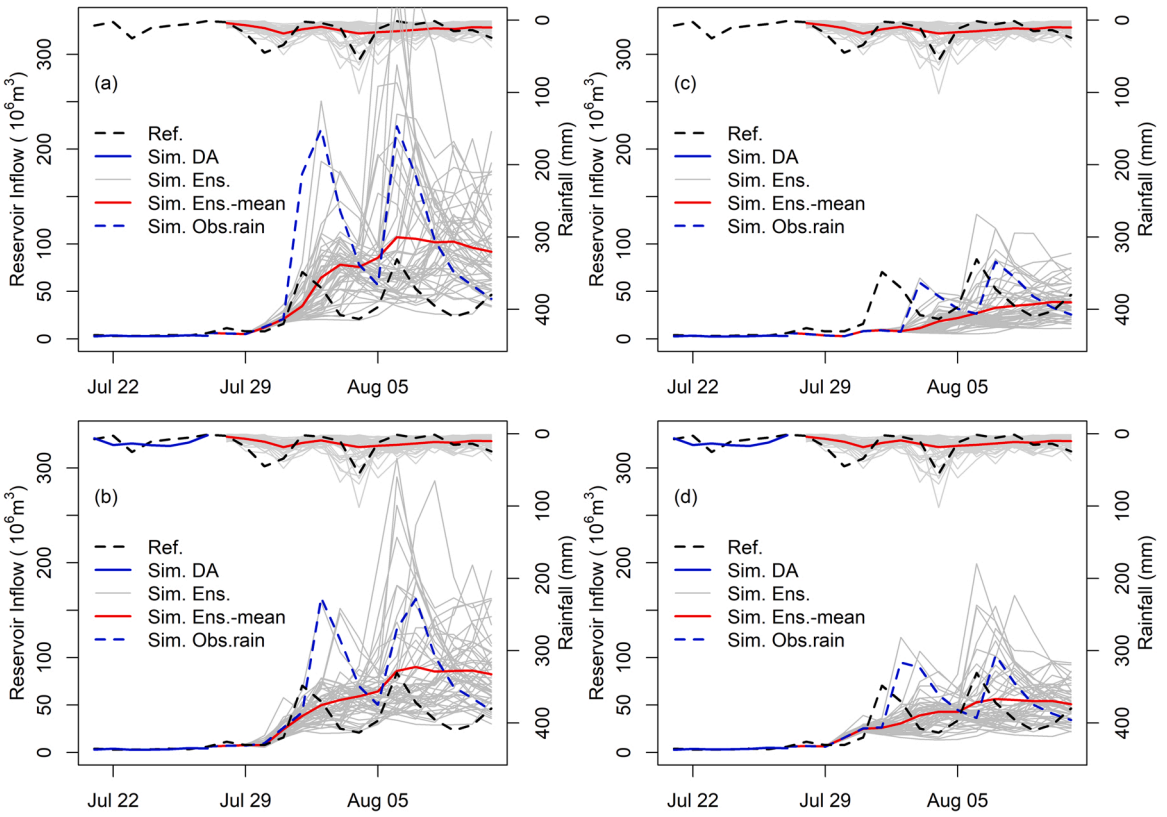

Fig. 11. Comparison of forecast hydrograph for simulation of week 31 among different forecast methods (a) method 1 (b) method 2 (c) method 3 and (d) method 4.

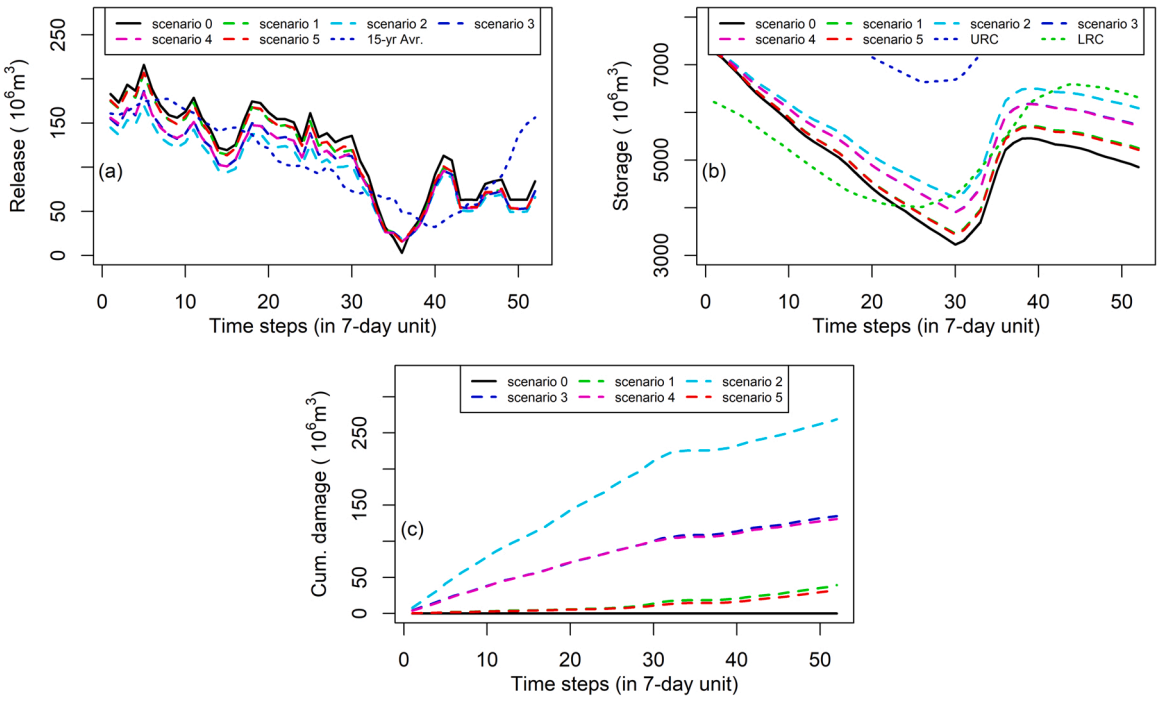

Fig. 12. Comparison of the Sirikit reservoir operation by adopting release strategies obtained from different scenarios of real-time optimization process.

Fig. 12b shows a comparison of the reservoir storage operated by the release strategies obtained from different optimization scenarios. Using an optimization process to determine the reservoir release decision, the reservoir storage at the end of 2019 was greater than that observed in operation (Scenario 0) for all scenarios. By associating forecast information in the real-time optimization of reservoir operation decision-making, such as scenarios 1−4, the overall reservoir water storage in 2019 is greater than that when predictions had not been considered (Scenario 5). Although Scenario 4 is considered as the perfect inflow forecast, there is no primary difference in the results obtained from Scenario 3. The forecast inflow for determining the release strategy in Scenario 3 has a similar tendency compared the actual inflow used in Scenario 4.

Fig. 12c presents a comparison of the accumulated total drought damage of the reservoir operation in different optimization scenarios. Although increased releases provided a smaller drought damage at the end of the year as the damage is a function of reservoir release, the remaining water budget for the future operation is different (difference in reservoir storage level at the end of the year). To compare the effectiveness of the optimization scenarios, the penalty might be considered for each storage level at the end of the year. This storage penalty can be calculated based on the future long-term inflow and the future demand assumptions using a backward calculation (Eq. (10)). For this study, we used the actual inflow in 2020 and the 50th percentile of the historical data in the dummy year. Thus, the penalties based on the end storage level for each scenario are summarized in Table 5.

The sum of the total drought damage in 2019 and end year storage penalty were the smallest for scenarios 3 and 4 and had the lowest value among all scenarios. Regarding the assumption of water demand, Scenario 0 (actual operation) had no damage in 2019. Considering end year storage penalty, it had the highest damage compared to all scenarios. Scenario 5 (without considering forecast) had the smallest drought damage in 2019 among optimization scenarios (scenarios 1−5), but resulted in the highest value when considering the storage penalty. Furthermore, we considered that the hydropower production was generated following the optimized release amount. Considering forecast information also resulted in a better potential of power generation as shown in Table 5. This demonstrates that there are advantages when associating forecast information with real-time optimization for decision-making in reservoir operation.

The future long-term inflow assumption (for penalty calculation) has a significant effect on the results of the reservoir operation. To improve optimization process efficiency, long-term forecasts with high performance should be utilized. In contrast, although the future long-term inflow is practically difficult to predict, the use of historical data, such as in scenarios 1 and 2, provided satisfactory results in this study.

7. Conclusions

This study presented a methodology to introduce ensemble weather forecast information collected from TIGGE archive data for real-time optimization of a 1-week advanced release strategy of the Sirikit reservoir, Thailand. The basin is located in a tropical climate region with a distinct wet and dry season, which has high uncertainty regarding hydrological conditions. This uncertainty increases challenges for reservoir operation. Despite the reservoir's operational challenges resulting from the high uncertainty regarding hydrological conditions in a tropical-climate basin, the case study indicated that reservoir operation would benefit by considering ensemble weather forecasts. Such reservoir operation improvements would have positive impacts for long-term hydropower generation and irrigation purposes. This result agrees with previous study in different regions that using forecast information with DP can support decision-making in water management (Faber and Stedinger, 2001; Kim et al., 2007; Nohara and Hori, 2018; Nohara et al., 2009).

Although this study indicates potential advantages of considering ensemble weather predictions for the 1-week advanced reservoir release strategy, there are some limitations. Firstly, the shortest time step of prediction can provide more advantages in reservoir operation such as floods control purposes. Secondly, further study may consider the forecast information such as temperature to

Table 5
Summary of reservoir operation result using release strategy obtained from different optimization scenarios.

Scenarios	Total release [million m^3]	End year storage [million m^3]	End year storage penalties*[million m^3]	Acc. drought damage [million m^3]		Hydropower production [GWh]	
				Within 2019	Including penalties*	Within 2019	Including future potential**
Scenario 0	6175.9	4851.0	624.6	0.0	624.6	1023.4	2618.4
Scenario 1	5770.0	5249.8	389.6	39.3	428.8	968.9	2629.7
Scenario 2	4914.4	6088.9	121.4	269.0	390.4	855.9	2681.0
Scenario 3	5289.3	5720.4	216.5	134.8	351.4	907.8	2656.3
Scenario 4	5297.7	5712.1	219.0	130.9	349.9	909.1	2655.6
Scenario 5	5804.8	5215.4	406.4	32.9	439.4	973.6	2628.7

*Possible min. drought damage at the end year storage level based on actual inflow in 2020 and Hist. p50 in dummy year.
**Potential of power generation at the end year storage level based on actual inflow in 2020 and Hist. p50 in dummy year.

predict the actual evapotranspiration rather than adopt historical data for improving inflow prediction. Thirdly, a real-time downstream water requirement may take into account for robust decision-making of long-term reservoirs. Fourthly, although this study demonstrated the advantages of the real-time reservoir optimization considering inflow predictions for a case study of 2019, the evaluation of the real-time scheme should be followed up with the further years. Lastly, this study presented significant differences in reservoir operation results driven by future long-term inflow assumptions (for a storage penalty estimation). Further studies might introduce long-range weather forecasts for more robust decision-making during reservoir operation.

By achieving the limitations, the real-time optimization scheme considering inflow predictions would be practically providing the benefit to society in terms of water resources management of the CPRB. In addition, this study illustrates the importance of TIGGE, which provides forecast data from various centers worldwide, which provides the benefits of research development in regions where these advanced products are scarce.

CRediT authorship contribution statement

Thatkiat Meema: Conceptualization, Methodology, Analysis, Software, Visualization, Writing – original draft. **Yasuto Tachikawa**: Supervision, Conceptualization, Methodology, Writing – review & editing. **Yutaka Ichikawa**: Conceptualization, Methodology. **Kazuaki Yorozu**: Conceptualization, Resources.

Declaration of Competing Interest

The authors declare that they have no known competing financial interests or personal relationships that could have appeared to influence the work reported in this paper.

Acknowledgements

This work is based on TIGGE data. TIGGE (The Interactive Grand Global Ensemble) is an initiative of the World Weather Research Programme (WWRP). We would like to acknowledge EGAT for providing the data information available on their website that made this study possible. This research was supported by Council for Science, Technology and Innovation (CSTI) of Japan, Cross-ministerial Strategic Innovation Promotion Program (SIP), “Enhancement of National Resilience against Natural Disasters” (Funding agency: National Research Institute for Earth Science and Disaster Resilience, NIED).

References

Alemu, E.T., Palmer, R.N., Polebitski, A., Meaker, B., 2011. Decision support system for optimizing reservoir operations using ensemble streamflow predictions. J. Water Resour. Plan. Manag. 137, 72–82. https://doi.org/10.1061/(asce)wr.1943-5452.0000088.

Alfieri, L., Thielen, J., Pappenberger, F., 2012. Ensemble hydro-meteorological simulation for flash flood early detection in southern Switzerland. J. Hydrol. 424–425, 143–153. https://doi.org/10.1016/j.jhydrol.2011.12.038.

Amnatsan, S., Yoshikawa, S., Kanae, S., 2018. Improved forecasting of extreme monthly reservoir inflow using an analogue-based forecasting method: A case study of the Sirikit Dam in Thailand. Water (Switzerland) 10. https://doi.org/10.3390/w10111614.

Bao, H.J., Zhao, L.N., He, Y., Li, Z.J., Wetterhall, F., Cloke, H.L., Pappenberger, F., Manful, D., 2011. Coupling ensemble weather predictions based on TIGGE database with Grid-Xinanjiang model for flood forecast. Adv. Geosci. 29, 61–67. https://doi.org/10.5194/adgeo-29-61-2011.

Bougeault, P., Toth, Z., Bishop, C., Brown, B., Burridge, D., De Chen, H., Ebert, B., Fuentes, M., Hamill, T.M., Mylne, K., Nicolau, J., Paccagnella, T., Park, Y.Y., Parsons, D., Raoult, B., Schuster, D., Dias, P.S., Swinbank, R., Takeuchi, Y., Tennant, W., Wilson, L., Worley, S., 2010. The thorpex interactive grand global ensemble. Bull. Am. Meteorol. Soc. 91, 1059–1072. https://doi.org/10.1175/2010BAMS2853.1.

Buizza, R., Bidlot, J.-R., Wedi, N., Fuentes, M., Hamrud, M., Holt, G., Vitart, F., 2007. The new ECMWF VAREPS (Variable Resolution Ensemble Prediction System). Q. J. R. Meteorol. Soc. 133, 681–695. https://doi.org/10.1002/qj.75.

Collischonn, W., Haas, R., Andreolli, I., Tucci, C.E.M., 2005. Forecasting River Uruguay flow using rainfall forecasts from a regional weather-prediction model. J. Hydrol. 305, 87–98. https://doi.org/10.1016/j.jhydrol.2004.08.028.

Duan, Q., Sorooshian, S., Gupta, V.K., 1994. Optimal use of the SCE-UA global optimization method for calibrating watershed models. J. Hydrol. 158, 265–284. https://doi.org/10.1016/0022-1694(94)90057-4.

Faber, B.A., Stedinger, J.R., 2001. Reservoir optimization using sampling SDP with ensemble streamflow prediction (ESP) forecasts. J. Hydrol. 249, 113–133. https://doi.org/10.1016/S0022-1694(01)00419-X.

Fan, F.M., Schwanenberg, D., Collischonn, W., Weerts, A., 2015. Verification of inflow into hydropower reservoirs using ensemble forecasts of the TIGGE database for large scale basins in Brazil. J. Hydrol. Reg. Stud. 4, 196–227. https://doi.org/10.1016/j.ejrh.2015.05.012.

Freeze, R.A., Cherry, J.A., 1979. Groundwater. Prentice-Hall. Inc., Englewood Cliffs, NJ.

Hamlet, A.F., Huppert, D., Lettenmaier, D.P, 2002. Economic value of long-lead streamflow forecasts for columbia river hydropower. J. Water Resour. Plan. Manag 128, 91–101. https://doi.org/10.1061/(asce)0733-9496(2002)128:2(91).

He, Y., Wetterhall, F., Bao, H., Cloke, H., Li, Z., Pappenberger, F., Hu, Y., Manful, D., Huang, Y., 2010. Ensemble forecasting using TIGGE for the July-September 2008 floods in the Upper Huai catchment: a case study. Atmos. Sci. Lett. 11, 132–138. https://doi.org/10.1002/asl.270.

Ikebuchi, S., Kojiri, T., Miyakawa, H., 1990. A study of long-term and real-time reservoir operation by using middle and long-term weather forecast. Annu. Disaster Prev. Res. Inst. Kyoto Univ. 33, 167–192 (in Japanese).

Kim, Y.-O., Eum, H.-I., Lee, E.-G., Ko, I.H., 2007. Optimizing operational policies of a Korean multireservoir system using sampling stochastic dynamic programming with ensemble streamflow prediction. J. Water Resour. Plan. Manag. 133, 4–14. https://doi.org/10.1061/(asce)0733-9496(2007)133:1(4).

Kotsuki, S., Tanaka, K., Watanabe, S., 2014. Projected hydrological changes and their consistency under future climate in the Chao Phraya River Basin using multi-model and multi-scenario of CMIP5 dataset. Hydrol. Res. Lett. 8, 27–32. https://doi.org/10.3178/hrl.8.27.

Lehner, B., Verdin, K., Jarvis, A., 2006. HydroSHEDS technical documentation version 1.0. World Wildlife Fund US, Washington, DC.

Lettenmaier, Wood, 1993. Hydrologic forecasting. In: Maidment (Ed.), Handbook of Hydrology. McGraw-Hill, New York.

Lin, J., Emanuel, K., Vigh, J.L., 2020. Forecasts of hurricanes using large-ensemble outputs. Weather Forecast. 35, 1713–1731. https://doi.org/10.1175/WAF-D-19-0255.1.

Loucks, D.P., Beek, E., van Stedinger, J.R., Dijkman, J.P.M., Villars, M.T., 2005. Water resources planning and management: an overview. In: Water Resources Systems Planning and Management An Introduction to Methods, Models and Applications.

Louoks, D.P., Falkson, L.M., 1970. A comparison of some dynamic, linear and policy iteration methods for reservoir operation. JAWRA J. Am. Water Resour. Assoc. 6, 384–400. https://doi.org/10.1111/j.1752-1688.1970.tb00489.x.

Madsen, H., Skotner, C., 2005. Adaptive state updating in real-time river flow forecasting - a combined filtering and error forecasting procedure. J. Hydrol. 308, 302–312. https://doi.org/10.1016/j.jhydrol.2004.10.030.

Meema, T., Tachikawa, Y., 2020. Structural improvement of a kinematic wave-based distributed hydrologic model to estimate long-term river discharge in a tropical climate basin. Hydrol. Res. Lett. 14, 104–110. https://doi.org/10.3178/hrl.14.104.

Moore, R.J., Bell, V.A., Jones, D.A., 2005. Forecasting for flood warning. C. R. Geosci. 337, 203–217. https://doi.org/10.1016/j.crte.2004.10.017.

Nguyen, H.T.T., Turner, S.W.D., Buckley, B.M., Galelli, S., 2020. Coherent streamflow variability in monsoon Asia over the past eight centuries—links to oceanic drivers. Water Resour. Res. 56 https://doi.org/10.1029/2020WR027883.

Nishimura, M., Yamaguchi, M., 2015. Selective ensemble mean technique for tropical cyclone track forecasts using multi-model ensembles. Trop. Cyclone Res. Rev. 4, 71–78. https://doi.org/10.6057/2015TCRR02.03.

Nohara, D., Hori, T., 2018. Reservoir operation for water supply considering operational ensemble hydrological predictions. J. Disaster Res. 13, 650–659. https://doi.org/10.20965/jdr.2018.p0650.

Nohara, D., Tsuboi, A., Hori, T., 2009. Long-term reservoir operation using one-month ensemble forecast of precipitation for introduction to a DSS, in: Proc. of 33rd IAHR Congress. IAHR, pp. 4215–4222.

O'Connell, P.E., Clarke, R.T., 1981. Adaptive hydrological forecasting—a review. Hydrol. Sci. Bull. 26, 179–205. https://doi.org/10.1080/02626668109490875.

Romanowicz, R.J., Young, P.C., Beven, K.J., 2006. Data assimilation and adaptive forecasting of water levels in the river Severn catchment, United Kingdom. Water Resour. Res. 42, 1–12. https://doi.org/10.1029/2005WR004373.

Sayama, T., Tatebe, Y., Iwami, Y., Tanaka, S., 2015. Hydrologic sensitivity of flood runoff and inundation: 2011 Thailand floods in the Chao Phraya River basin. Nat. Hazards Earth Syst. Sci. 15, 1617–1630. https://doi.org/10.5194/nhess-15-1617-2015.

Sayama, T., Yamada, M., Sugawara, Y., Yamazaki, D., 2020. Ensemble flash flood predictions using a high-resolution nationwide distributed rainfall-runoff model: case study of the heavy rain event of July 2018 and Typhoon Hagibis in 2019. Prog. Earth Planet. Sci. 7 https://doi.org/10.1186/s40645-020-00391-7.

Takeda, M., Laphimsing, A., Putthividhya, A., 2016. Dry season water allocation in the Chao Phraya River basin, Thailand. Int. J. Water Resour. Dev. 32, 321–338. https://doi.org/10.1080/07900627.2015.1055856.

Tanaka, T., Tachikawa, Y., 2015. Testing the applicability of a kinematic wave-based distributed hydrological model in two climatically contrasting catchments. Hydrol. Sci. J. 60, 1361–1373. https://doi.org/10.1080/02626667.2014.967693.

Tingsanchali, T., Boonyasirikul, T., 2006. Stochastic dynamic programming with risk consideration for transbasin diversion system. J. Water Resour. Plan. Manag. 132, 111–121. https://doi.org/10.1061/(asce)0733-9496(2006)132:2(111).

Weber, H.C., 2003. Hurricane track prediction using a statistical ensemble of numerical models. Mon. Weather Rev. 131, 749–770. https://doi.org/10.1175/1520-0493(2003)131<0749:HTPUAS>2.0.CO;2.

Wichakul, S., Tachikawa, Y., Shiiba, M., Yorozu, K., 2015. River discharge assessment under a changing climate in the Chao Phraya River Thailand by using MRI-AGCM3.2S. Hydrol. Res. Lett. 9, 84–89. https://doi.org/10.3178/hrl.9.84.

Zenkoji, S., Tebakari, T., Dotani, K., 2019. Rainfall and reservoirs situation under the worst drought recorded in the Upper Chao Phraya River Basin, Thailand. J. Japan Soc. Civ. Eng. Ser. G (Environmental Res.). 75, I_115–I_124. https://doi.org/10.2208/jscejer.75.i_115.

Zhu, Y., 2005. Ensemble forecast: a new approach. Adv. Atmos. Sci. 22, 781–788.

Zhu, Y., Toth, Z., Wobus, R., Richardson, D., Mylne, K., 2002. The economic value of ensemble-based weather forecasts. Bull. Am. Meteorol. Soc. 83, 73–83. https://doi.org/10.1175/1520-0477(2002)083<0073:TEVOEB>2.3.CO;2.